BUTTERWORTH HEINEMANN

Polymer Vol. 36 No. 23, pp. 4453–4462, 1995
Copyright © 1995 Elsevier Science Ltd
Printed in Great Britain. All rights reserved
0032-3861/95/$10.00+0.00

Comparison of compatibilizer effectiveness for PET/HDPE blends

Nikos K. Kalfoglou*, Dimitrios S. Skafidas and Joannis K. Kallitsis
Department of Chemistry, University of Patras, 26500 Patras, Greece

and Jean-Claude Lambert and Luc Van der Stappen
CRIF-MATERIAUX, Plastic Materials Division B-4000 Liege, Belgium
(Received 13 October 1994; revised 5 April 1995)

The efficiency of four different compatibilizers melt-mixed with a poly(ethylene terephthalate)/high density polyethylene (PET/HDPE) blend was investigated. The compatibilizers studied were an ethylene–glycidyl methacrylate copolymer (E-GMA), an ethylene ethylacrylate glycidyl methacrylate terpolymer (E-EA-GMA), a hydrogenated styrene–butadiene–styrene copolymer grafted with maleic anhydride (SEBS-*g*-MA) and a MA-modified ethylene–methyl acrylate copolymer (E-MeA-*g*-MA). The techniques applied were dynamic mechanical analysis, tensile and impact testing, optical and electron microscopy, thermal analysis and Fourier transform infra-red spectroscopy. On the basis of morphological evidence and tensile testing, which proved most discriminating, the compatibilizing effectiveness was found to decrease in the sequence, E-GMA> E-EA-GMA> SEBS-*g*-MA>E-MeA-*g*-MA. These results are explained on the basis of differing reactivities of the GMA vs. the MA functionality contained in these compatibilizers.

(Keywords: compatibilization; compatibilizer efficiency; PET/HDPE blends)

INTRODUCTION

Current environmental policies for pollution abatement and raw material conservation encourage the recycling of plastics[1–3]. Among them, polyolefins (PO) and poly(ethylene terephthalate) (PET) have attracted considerable research activity since large amounts are available through recycling technology.

In the area of polymer blends, the challenge is to recycle mixed plastics, at the same time maintaining an acceptable level of properties and cost. In this context the study of PET/PO blends is of considerable technological importance. Given the fact that this binary blend is incompatible[4], research efforts have been directed towards PET modification or compatibilization of its blend with PO.

Previous work on reactive PET modification includes the report by Wu[5], who examined the interfacial and rheological factors affecting the state of dispersion of ethylene–propylene rubber (EPR) without and with a reactive functionality (probably maleic anhydride). A related system was examined by Yokoyama *et al.*[6] who reported on morphology evolution and interface thickness variation during melt-mixing. Subramanian[7,8] reported on the toughness, morphology, crystallinity and permeability of PET/ionomer blends using a variety of ionomers at a single composition. The toughening of PET with ethylene–glycidyl methacrylate copolymer (E-GMA) and with its ethyl acrylate terpolymer (E-EA-GMA) was investigated by Akkapeddi and Van Buskirk[9], who investigated the effects of processing conditions and thermal treatment. We have recently reported[10] on the compatibility of PET melt-mixed with the ionomer salt of ethylene–methacrylic acid copolymer in the complete composition range. We have also reported[11] on the compatibilization of PET/linear low density polyethylene (LLDPE) using as compatibilizer the ionomer of ethylene methacrylic acid copolymer. Good mechanical properties of quenched blends were obtained at moderate levels of the compatibilizer and at increased levels of PET.

Work related to the effectiveness of various compatibilizers for PET/PO blends includes the findings of Paul and co-workers[12] who used a hydrogenated styrene–butadiene–styrene triblock copolymer (SEBS) and an ethylene–propylene–diene elastomer (EPDM). Improved ductility was reported using SEBS only. Curry and Kiani[13] used a maleic anhydride grafted PE (PE-*g*-MA) and a styrene–ethylene propylene block copolymer, and found better mechanical performance with the former. Wissler[14] compared various ethylene copolymers (esters and acrylic acid) as compatibilizers directly or with grafting agents, and in the latter case found toughness improvement. Lately, Carte and Moet published[15] their findings on the morphology and impact properties of PET/high density polyethylene (HDPE) compatibilized with SEBS, SEBS-*g*-MA and HDPE-*g*-MA. Best results were obtained with modified SEBS.

In this work, the mechanical, thermal and morphological features of a PET/HDPE blend compatibilized with four chemically different compatibilizers are examined. Where required, some PET/compatibilizer blends were

---

* To whom correspondence should be addressed

also studied to characterize the degree of component interaction. Blends were prepared by melt-mixing PET/HDPE/compatibilizer at the composition 70/20/10, using as compatibilizers E-GMA, E-EA-GMA, SEBS-*g*-MA and an anhydride-modified ethylene methyl acrylate resin (E-MeA-*g*-MA). Mechanical properties studied were tensile, impact and dynamic. Thermal analysis by differential scanning calorimetry (d.s.c.) was applied to determine the crystallinity of PET and melting transitions. Morphology examination covered optical microscopy (phase contrast, polarizing) and scanning electron microscopy (SEM) on fractured and etched specimens. Fourier transform infra-red (*FT*i.r.) spectroscopy was also applied to determine component interaction in cases where peak resolution of the main components in the binary PET/compatibilizer blends was possible.

EXPERIMENTAL

Materials and compounding

PET was a recycled grade ('Retech', origin SPA (Belgium), bottles) of high purity (5 ppm non-solubles, 50 ppm polyolefins) with molecular characteristics close to those of virgin PET (Arnite DO2 300, AKZO b.v.). $\bar{M}_n$ was reported to be 22 000 g mol^{-1}, $\bar{M}_w/\bar{M}_n = 2.7$ and intrinsic viscosity (*IV*) in tetrachloroethane/phenol

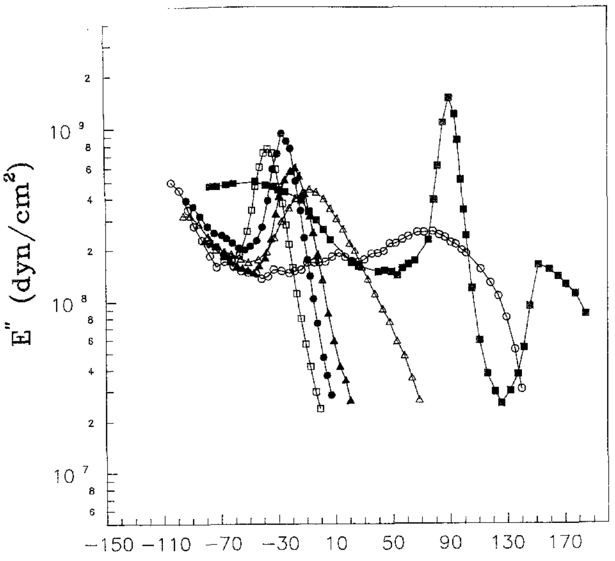

Figure 1 Temperature dependence of loss modulus of homopolymers: (■) PET; (○) HDPE; (△) E-GMA; (▲) E-MeA-*g*-MA; (●) E-EA-GMA; (□) SEBS-*g*-MA

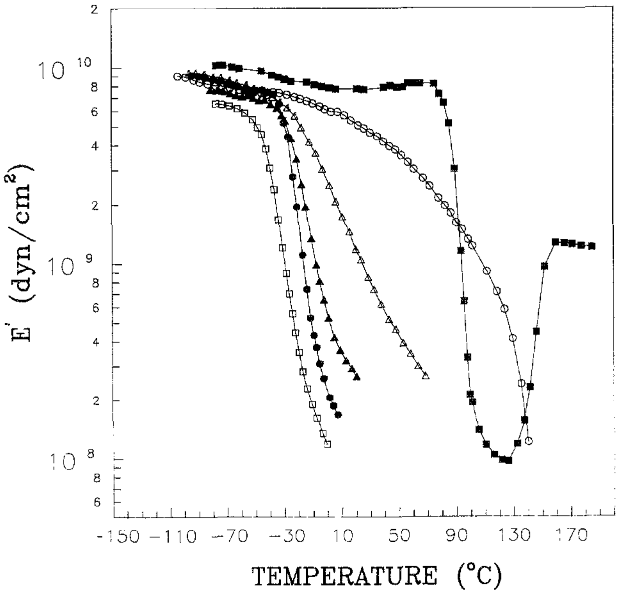

Figure 2 Temperature dependence of storage modulus of homopolymers: (■) PET; (○) HDPE; (△) E-GMA; (▲) E-MeA-*g*-MA; (●) E-EA-GMA; (□) SEBS-*g*-MA

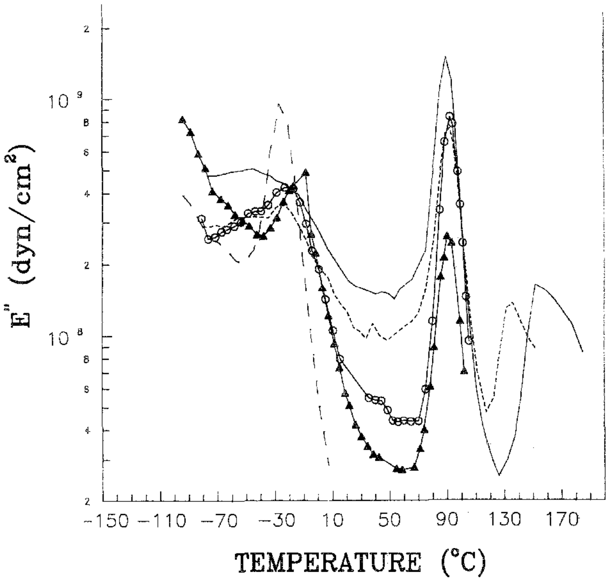

Figure 3 Composition dependence of loss modulus of PET/E-EA-GMA binary blends: (—)100/0; (○) 75/25; (▲) 50/50; (– –) 0/100; (----) ternary blend

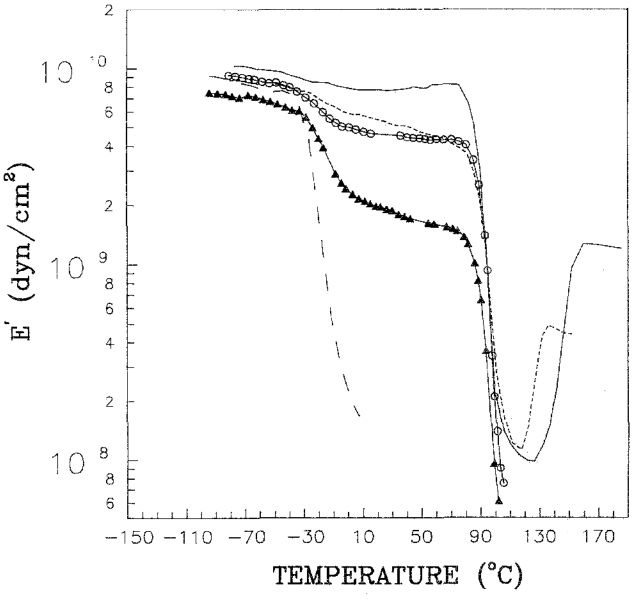

Figure 4 Composition dependence of storage modulus of PET/E-EA-GMA binary blends: (—)100/0; (○) 75/25; (▲) 50/50; (– –) 0/100; (----) ternary blend

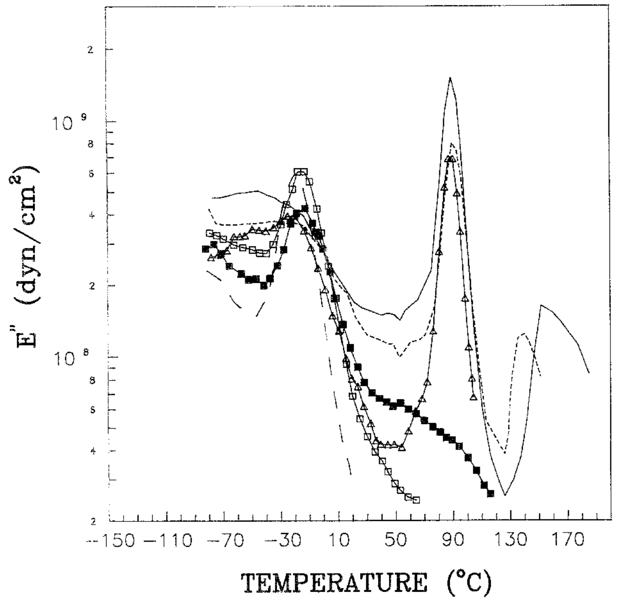

Figure 5 Composition dependence of loss modulus of PET/E-MeA-*g*-MA binary blends: (—)100/0; (△) 75/25; (□) 50/50. HDPE/E-MeA-*g*-MA binary: (■) 50/50; (---) ternary blend

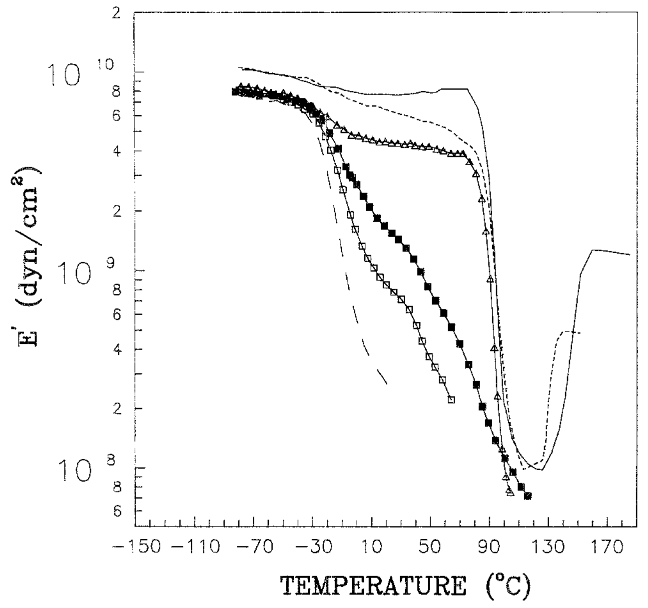

Figure 6 Composition dependence of storage modulus of PET/E-MeA-*g*-MA binary blends: (—)100/0; (△) 75/25; (□) 50/50. HDPE/E-MeA-*g*-MA binary: (■) 50/50; (---) ternary blend

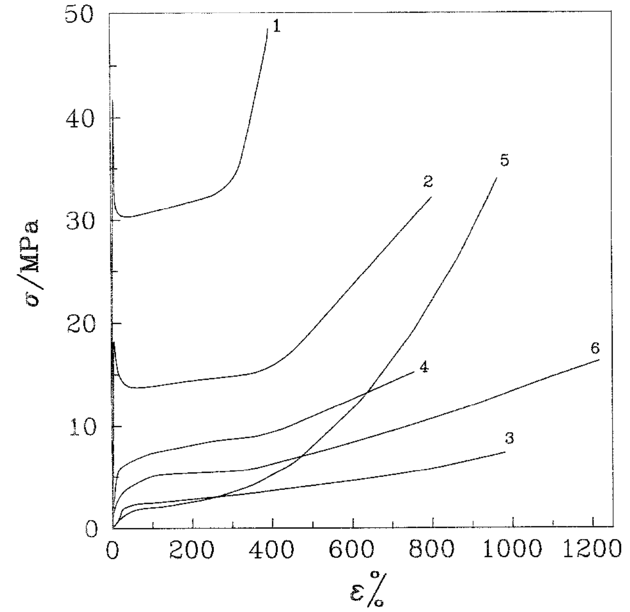

Figure 7 Stress–strain properties of homopolymers: 1, PET; 2, HDPE; 3, E-EA-GMA; 4, E-GMA; 5, SEBS-*g*-MA; 6, E-MeA-*g*-MA

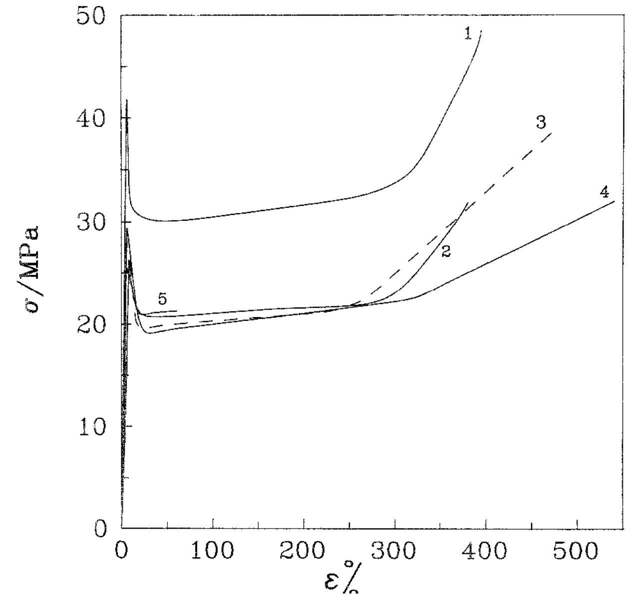

Figure 8 Stress–strain properties of ternary blends with indicated compatibilizers: 1, PET homopolymer; 2, E-EA-GMA; 3, E-GMA; 4, SEBS-*g*-MA; 5, E-MeA-*g*-MA

mixture was 0.78. Virgin PET had $\bar{M}_n = 24\,000\,g\,mol^{-1}$, $\bar{M}_w/\bar{M}_n = 2.04$ and $IV = 0.73$. Neither dynamic mechanical nor tensile properties indicated essential differences between the two grades within the experimental accuracy. HDPE (Finathene 47100) was obtained from Petrofina S.A. (Belgium). It is a blow-moulding grade with density $0.945\,g\,cm^{-3}$ and melt flow index 8–12 g/10 min (190°C/21.6 kg). The compatibilizers used were an E-EA-GMA terpolymer (Lotader AX8660) and an E-GMA copolymer (Lotader AX 8840), both from Atochem Co. (France); a SEBS-*g*-MA (Kraton FG 1901X) from Shell Chemical Co. (with 29 wt% styrene and MA content of 1.84 wt%); and an E-MeA-*g*-MA copolymer (Bynel CXA E369) from DuPont, with MA content determined to be 1.40 wt%.

PET was dried in a dehumidifying air drier at up to 160°C for 8 h. HDPE and the compatibilizers were dried at temperatures of 120 and 80°C, respectively. The dried materials were tumble-blended and fed into a ZSK twin co-rotating, intermeshing screw extruder operating at a temperature profile of 251–281–281–282–279°C, a feed rate of $55\,kg\,h^{-1}$ at $170\,rev\,min^{-1}$. The extrudate was cooled and stranded in a water bath before pelletization. After the final drying, the moisture level was less than 0.01%.

Experiments established that the screw configuration

Table 1 Ultimate properties of polymers and blends[a]

Polymer	σ_b (MPa)	σ_y (MPa)	ϵ_b (%)	E_b (J cm^{-3})
PET ('Arnite')	48 ± 3	42 ± 3	410 ± 20	134
PET ('Retech')	42 ± 3	42 ± 2	390 ± 30	–
HDPE	32 ± 3	18 ± 2	800 ± 50	149
E-EA-GMA	7 ± 1	–	980 ± 50	41
E-GMA	15 ± 0.5	–	750 ± 40	75
SEBS-*g*-MA	34 ± 3	–	960 ± 30	104
E-MeA-*g*-MA	16 ± 1	–	1220 ± 100	105
E-EA-GMA blend	32 ± 2	26 ± 0.5	380 ± 50	84
E-GMA blend	39 ± 3	27 ± 0.5	480 ± 30	115
SEBS-*g*-MA blend	32 ± 4	22 ± 1	540 ± 30	123
E-MeA-*g*-MA blend	21 ± 2	29 ± 0.5	65 ± 25	12
E-EA-GMA blend[b]	29 ± 1	27 ± 1	310 ± 90	–
E-GMA blend[b]	29 ± 2	25 ± 1	420 ± 30	–

[a] Quenched (0°C), vacuum dried
[b] Air oven dried

Table 2 Impact properties[a]

Polymer or blend	Impact strength (kJ m^{-2})
PET ('Arnite')	4.0 ± 0.3
PET ('Retech')	4.4 ± 1.1
E-EA-GMA blend	8.3 ± 1.0
E-EA-GMA blend[b]	12.0 ± 5
E-GMA blend	30 ± 2
E-GMA blend[b]	34 ± 7
SEBS-*g*-MA blend	9.6 ± 1
E-MeA-*g*-MA blend	9.4 ± 1

[a] Vacuum oven dried
[b] Air oven dried

Table 3 Thermal transitions and crystallinity of PET in blends

Blend	T_m PET (°C)	T_c[a] (°C)	Crystallinity PET (%)
E-EA-GMA	247	119	17.8
E-GMA	247	–	17.5
SEBS-*g*-MA	247	127	18.2
E-MeA-GMA	247	126	21.3
PET 'Retech'	248	126	24.4

[a] From d.m.a. data

(co- vs. counter-rotating) and the use of the compatibilizer as received (vs. vacuum drying before mixing) did not have any effect on the mechanical properties of the blends.

Bars for impact tests were injection-moulded with a Billion 90 ton injection moulder (barrel temperatures spanning the range 255–280°C) with the mould at 40°C. Films for tensile tests, dynamic mechanical analysis (d.m.a.) and d.s.c. were prepared by compression-moulding between Teflon sheets at ~ 275°C, 15 MPa and quenching to 0°C.

In the following, since only the type of compatibilizer is varied in the ternaries, they will be characterized by the name of this component; thus an E-GMA ternary signifies a blend of PET/HDPE/E-GMA at a weight ratio 70/20/10, the weight ratio being constant for all ternaries. When two-component blends are referred to they will be specified as binaries.

Apparatus and procedures

The d.m.a. data loss tangent (tan δ) and complex modulus $|E^*|$ were obtained at 110 Hz using a direct-reading viscoelastometer (Rheovibron DDV II-C). Specimen dimensions were 3.0 cm × 0.25 cm × 0.03 cm. Tensile tests were performed according to ASTM D882 using a J.J. Tensile Tester type T5001 and film strips with dimensions 6.0 cm × 1.0 cm × 0.05 cm. Crosshead speed was 10 cm min^{-1}.

Impact tests were performed according to Charpy DIN 53453, normal piece, notched, using a Zwick pendulum impact tester model 5101. D.s.c. measurements were carried out in an inert atmosphere using a DuPont 910 calorimeter system coupled with a 990 programmer recorder. Sample weight was ~10 mg and heating rate was 10°C min^{-1} to obtain thermal transitions, and 20°C min^{-1} to determine crystallinity.

Optical micrographs were obtained with an Olympus BH-2 microscope. Specimens prepared by melt-pressing between a cover glass and a microscope slide were quenched to 25°C. SEM was a JEOL model JSM-5200. Fractured surfaces at cryogenic and ambient temperatures, or after microtoming and etching with boiling toluene (8 h), were examined at a tilt angle of 30°. *FT*i.r. spectra were obtained using a Perkin–Elmer 1600 spectrometer.

RESULTS

Mechanical properties

The dynamic viscoelastic spectra of the quenched (0°C) pure blend components are shown in *Figures 1* and *2*, in terms of the temperature dependence of the loss E'' and storage E' modulus, respectively. The main relaxations of PET are located at 90°C (α) and −50°C (β). They have been associated[16] with the amorphous component and are strongly dependent on crystallinity. HDPE has its broad α relaxation[17] centred around 75°C. All of the compatibilizers have a main glass transition relaxation at sub-zero temperatures: E-GMA at −8°C, E-MeA-*g*-MA

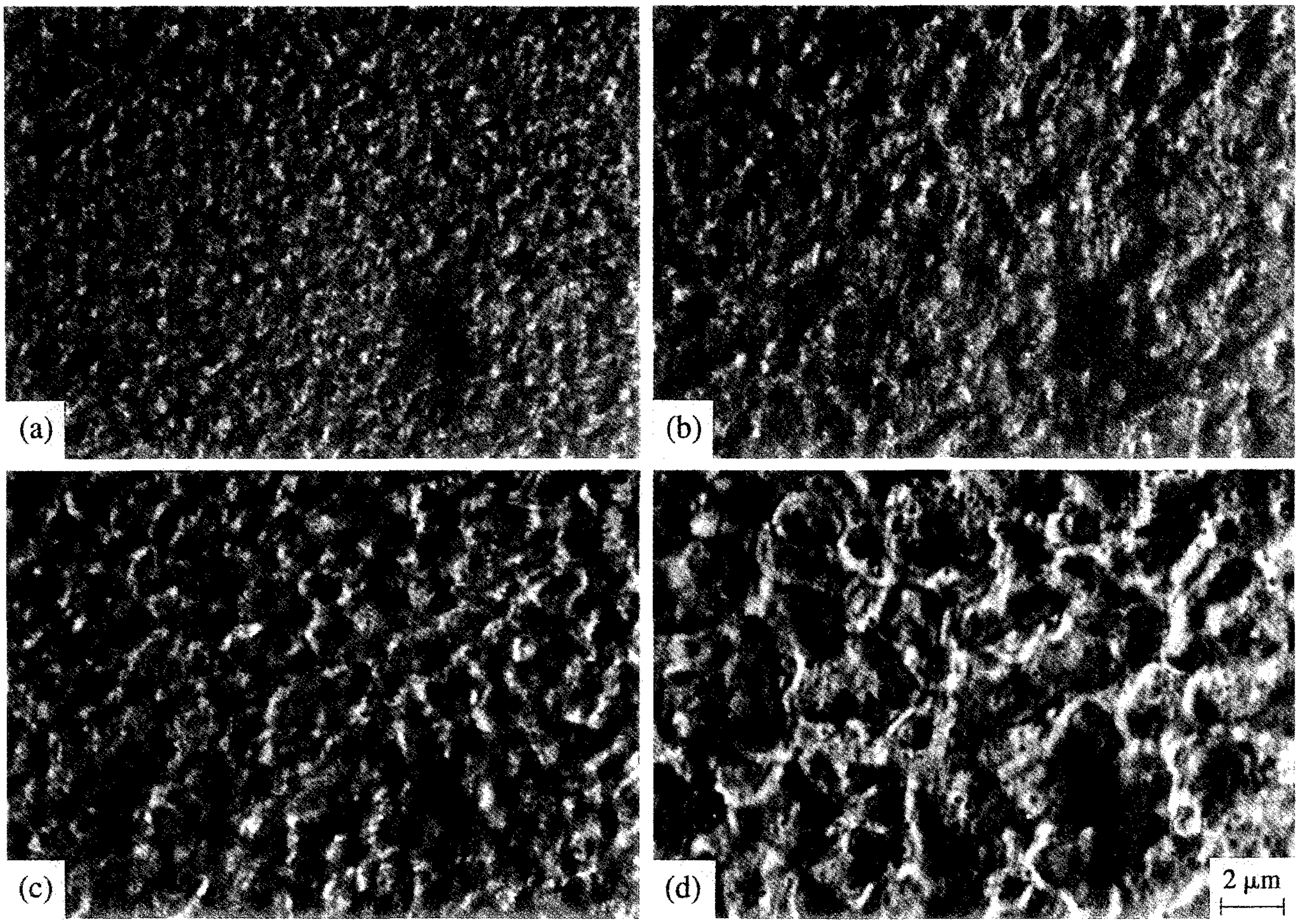

Figure 9 Phase-contrast micrographs of ternary blends with indicated compatibilizers: (a) E-GMA; (b) E-EA-GMA; (c) SEBS-*g*-MA; (d) E-MeA-*g*-MA

at −18°C, E-EA-GMA at −28°C and the SEBS-*g*-MA at −36°C. Correspondingly, the modulus drop takes place at progressively lower temperatures (see *Figure 2*). For PET, the cold crystallization onset at above ~ 120°C is also seen as an increase in E'.

To demonstrate a possible PET/compatibilizer interaction, the effect on main transitions of varying the composition of these binaries was examined, and typical d.m.a. results are shown in *Figures 3* and *4* for the PET/E-EA-GMA binary blend. For this system, which was the most thoroughly studied, a small systematic shift of the PET (α) and the E-EA-GMA (β) relaxations towards each other was observed with increasing compatibilizer content. For the 50/50 composition, the α is reduced from 93 to 90°C and the β shifted from −28 to −17°C (see *Figure 3*). However, main relaxations are conserved. This and the modulus drop in *Figure 4* are characteristic of a heterophase blend with limited mixed interphase formation[18]. Similar features with smaller shifts were observed for the PET/SEBS-*g*-MA and the PET/E-MeA-*g*-MA binary blends (*Figures 5* and *6*, where only the latter is depicted). In the last case, based on the E'' spectrum, the 50/50 composition suggests miscibility since a single relaxation at around −17°C is observed. However, modulus variation (*Figure 6*) shows two steps, indicating a phase-separated system. Superimposed on these spectra are the data of the ternary blend for the corresponding compatibilizer. The ternaries retain the features of a phase-separated blend. The relaxation shifts, however, are smaller due to dilution (addition of HDPE). It is of interest to note the modulus stiffening in the ternaries compared to the corresponding 75/25 binaries (*Figure 6*). The effect is strongest for the SEBS-*g*-MA ternary.

Tensile properties

Tensile properties refer to stress–strain (σ–ϵ), ultimate strength and elongation, σ_b and ϵ_b, respectively, and energy to tensile failure, E_b, obtained as the area under the σ–ϵ curve. Of these, elongation at break, ϵ_b, is very sensitive to blend component adhesion strength[19] and is routinely used to evaluate the degree of compatibilization in polymer alloys[20]. *Figure 7* records the stress–strain curves of the pure quenched components. The curves of the compatibilizers are typical of soft, flexible materials with no yield point, except for SEBS-*g*-MA whose PS blocks impart a self-reinforcing character. The tensile properties of the ternaries are shown in *Figure 8*, compared to pure PET. All show good elongation and strength except for the E-MeA-*g*-MA ternary. These data and E_b values are summarized in *Table 1*. *Table 1* also compares the effect of vacuum oven drying vs. air oven drying for two ternaries having epoxy-containing compatibilizers. A minor property deterioration is evident, possibly the result of crosslinking in the air oven.

Impact properties

Impact properties are given in *Table 2*, where the effect

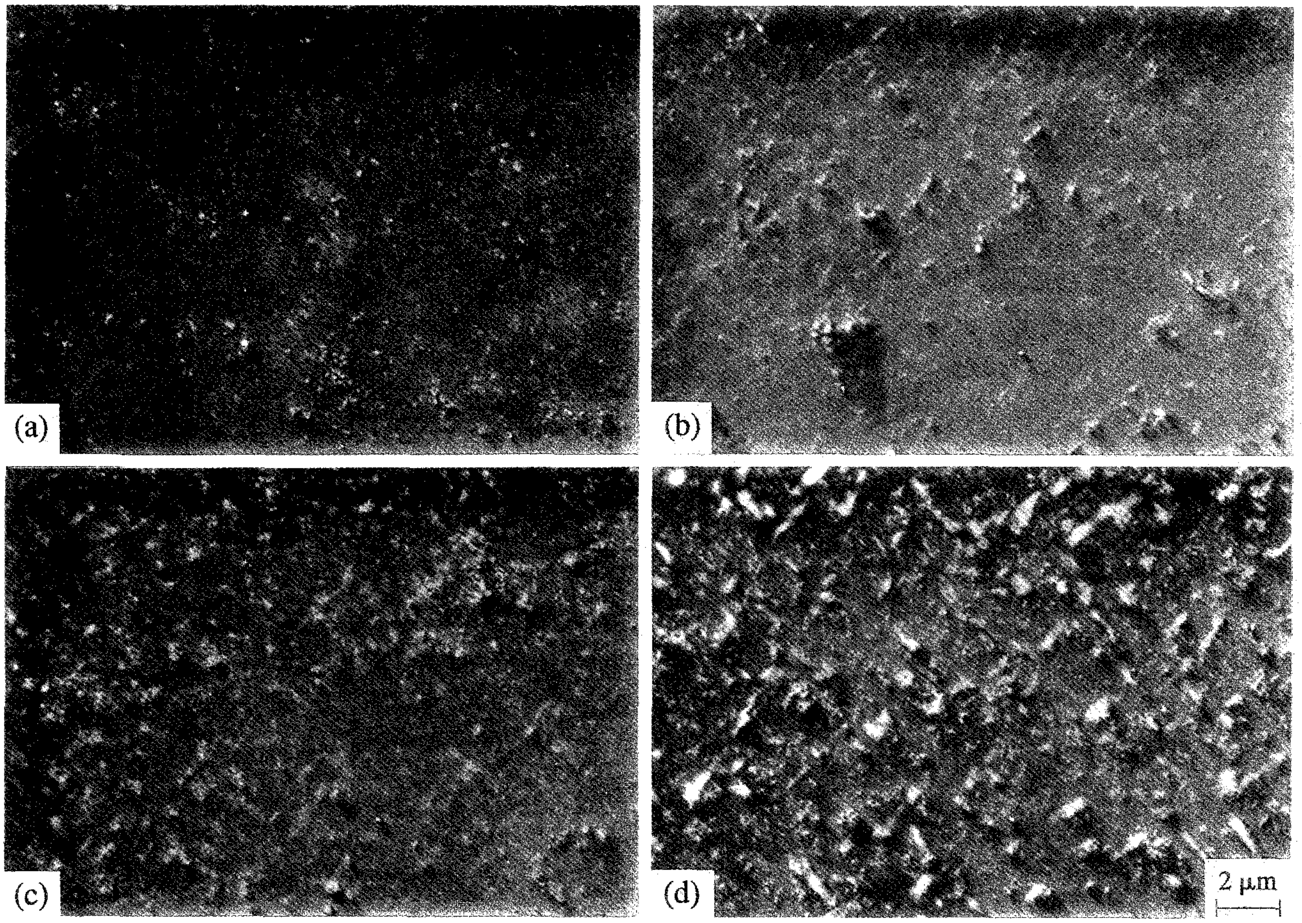

Figure 10 Optical micrographs with crossed polars of ternary blends with indicated compatibilizers: (a) E-GMA; (b) E-EA-GMA; (c) SEBS-*g*-MA; (d) E-MeA-*g*-MA

of drying in vacuum and air ovens is also reported. Best properties are obtained with E-GMA as compatibilizer. Though chemically related, E-EA-GMA is grouped with the rest of the compatibilizers showing the same level of impact strength. The difference in impact–tensile ternary differentiation is attributed to differing procedures of specimen preparation and mode of deformation in the two techniques (see also Discussion and Conclusions). It should be pointed out that while the E-MeA-*g*-MA is a very poor compatibilizer on the basis of tensile deformation, it is equally good as SEBS-*g*-MA and E-EA-GMA on the basis of impact ternary performance. The effect of air oven drying is to raise impact strength at the expense of property reproducibility. Again, crosslinking may account for the results.

Thermal properties

Thermal properties are reported in *Table 3* and refer to the melting temperature (T_m) of PET and its crystallinity developed during the heating scan. The corresponding data for the HDPE component could not be determined because of the onset at the crystallization temperature (T_c) of cold crystallization interference by PET. The results on crystallinity suggest that its development is less hindered in the case of E-MeA-*g*-MA ternary, indicating a less intimate phase mixing in line with morphology findings.

Morphology

Optical microscopy. Figure 9 gives the phase-contrast micrographs of the ternaries. Given the refractive index of PET and PO, at positive phase contrast the dark and light areas should correspond to the PET and PO component, respectively. The ternaries show an interpenetrating phase distribution at the sub-micrometre level (except for the E-MeA-*g*-MA blend). Dispersion becomes coarser in the order E-GMA, E-EA-GMA, SEBS-*g*-MA and poorest distribution is shown by the E-MeA-*g*-MA ternary. *Figure 10* shows micrographs obtained with crossed polars. While PET may be quenched to the glassy state (dark area), the PO phase crystallizes too fast to pass into the amorphous glassy state. Thus white areas represent PO crystalline domains. These become finer for the well dispersed E-GMA ternary blend (*Figure 10a*), while the gross phase distribution in the E-MeA-*g*-MA ternary allows the development of larger crystalline domains (*Figure 10d*).

Scanning electron microscopy (SEM). Three sets of specimen surfaces were examined: (i) impact-fractured at ambient temperature (*Figure 11*); (ii) cryofractured (*Figure 12*); (iii) microtomed and etched with boiling toluene (8 h) (*Figure 13*). This treatment would remove any non-grafted compatibilizer plus most of the PO phase. Examination of *Figure 11* shows a tough type of fracture proceeding almost entirely within the matrix (*Figure 11a* and *b*). Some particles strongly adhering onto the matrix are also discernible (*Figure 11b*). *Figure 11c* and *d* show features of mixed ductile–brittle fracture with particles dislodged from the matrix. This feature is most evident in *Figure 11d*, the E-MeA-*g*-MA ternary

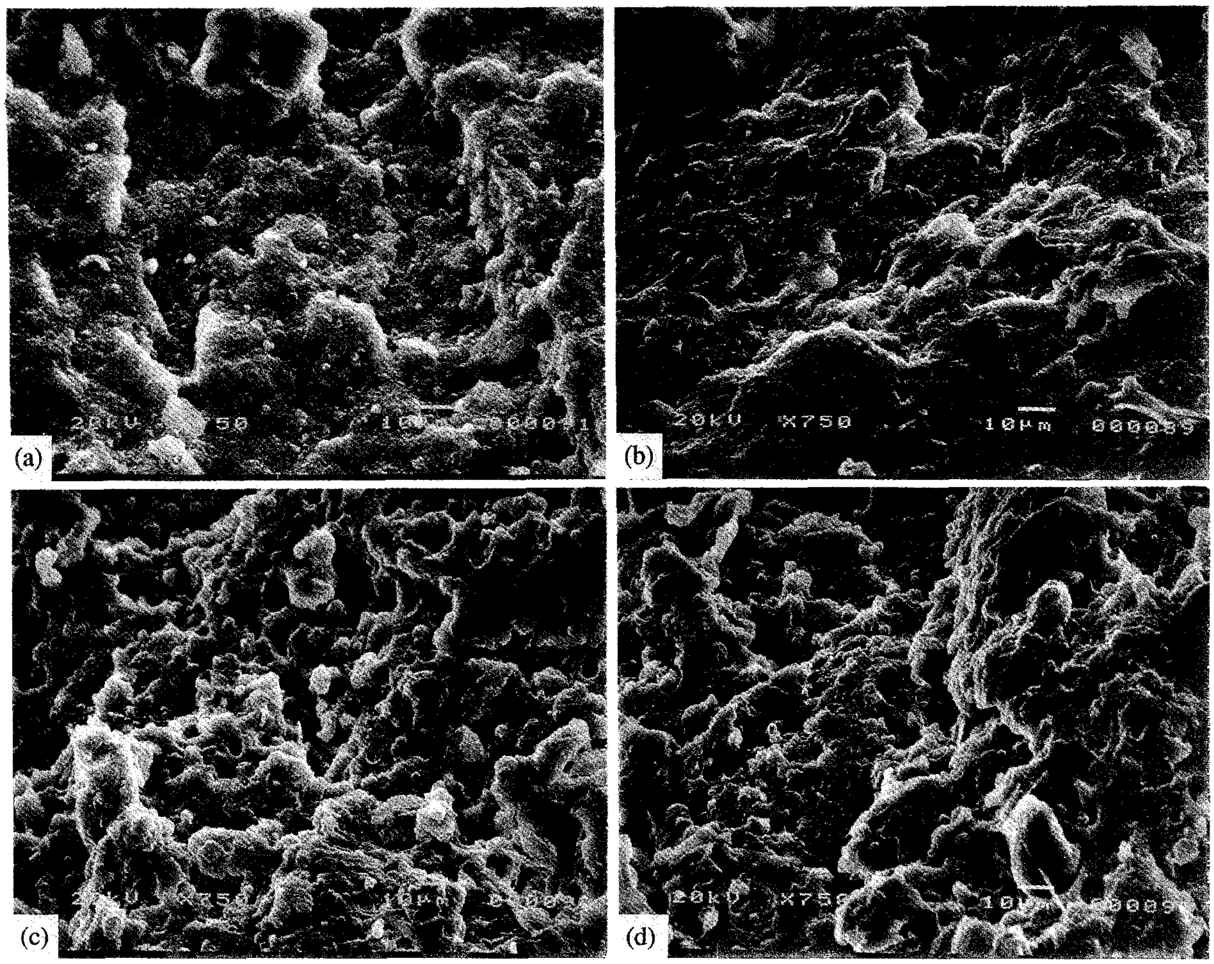

Figure 11 SEM micrographs of impact-fractured ternary blends with indicated compatibilizers: (a) E-GMA; (b) E-EA-GMA; (c) SEBS-*g*-MA; (d) E-MeA-*g*-MA

blend. Micrographs in *Figure 12* show similar trends, and the distinctly tough type of fracture is seen in the case of the E-GMA ternary blend (*Figure 12a*). In etched surface micrographs (*Figure 13*) it is clear that the HDPE+compatibilizer (removed by toluene) has been finely dispersed and interlocked with the PET matrix in the E-GMA ternary (*Figure 13a*). A progressively coarser phase distribution is evident along the series E-EA-GMA (*Figure 13b*) and SEBS-*g*-MA (*Figure 13c*), while a very poor dispersion is shown in the E-MeA-*g*-MA ternary (*Figure 13d*), with no evidence of phase interlocking. These SEM results are in line with optical microscopy and explain the poor tensile properties of the E-MeA-*g*-MA ternary blend. This is reasonable, since good component adhesion in polymer alloys depends on the interface area between them, which decreases along the ternary blend series E-GMA>E-EA-GMA>SEBS-*g*-MA>>E-MeA-*g*-MA.

FT*i.r. characterization*

The spectroscopic investigation of blends aimed at establishing the reaction of the glycidyl epoxy groups of the compatibilizers (E-EA-GMA, E-GMA) with the OH and COOH groups of PET according to *Scheme 1*[21,22].

The glycidyl epoxy group absorbs at 912 cm^{-1}. This was confirmed by ring scission after reacting with HBr in CH_3COOH and reexamination of the product obtained. The 912 cm^{-1} absorption is absent and an absorption due to α-bromoalcohol at 3502 cm^{-1} is obtained. Studies were concentrated mainly on the PET/E-GMA binary because of its simpler structure. PET/E-GMA binaries at 90/10 and 70/30 were melt-mixed in a glass reactor (in inert atmosphere). E-GMA itself was also melt-treated under similar conditions since it may, in principle, undergo crosslinking reactions. *Figures 14a–d* show the spectra of pure components and their blend. The oxirane absorption at 912 cm^{-1} disappears in the blend (*Figure 14d*). It is also significant that the peak ratio 874 cm^{-1}/846.6 cm^{-1} of pure PET (*Figure 14a*), is altered in the case of blends, indicating the formation of a new chemical species. Since E-GMA remains unaltered after heat treatment (compare *Figures 14b* and *c*), the disappearance of the 912 cm^{-1} absorption in blends is evidence for the oxirane reacting with PET as in *Scheme 1*. The same reaction is expected to proceed in the ternary as well, the HDPE acting as an inert diluent. *FT*i.r. studies of blends with the other types of compatibilizers could not give clear evidence for component reaction, because the PET carbonyl absorption interfered with the absorption bands of MA (and its reaction products) appearing in the same range.

DISCUSSION AND CONCLUSIONS

To classify the compatibilizer effectiveness in this reactive extrusion process (REX)[21] one should take

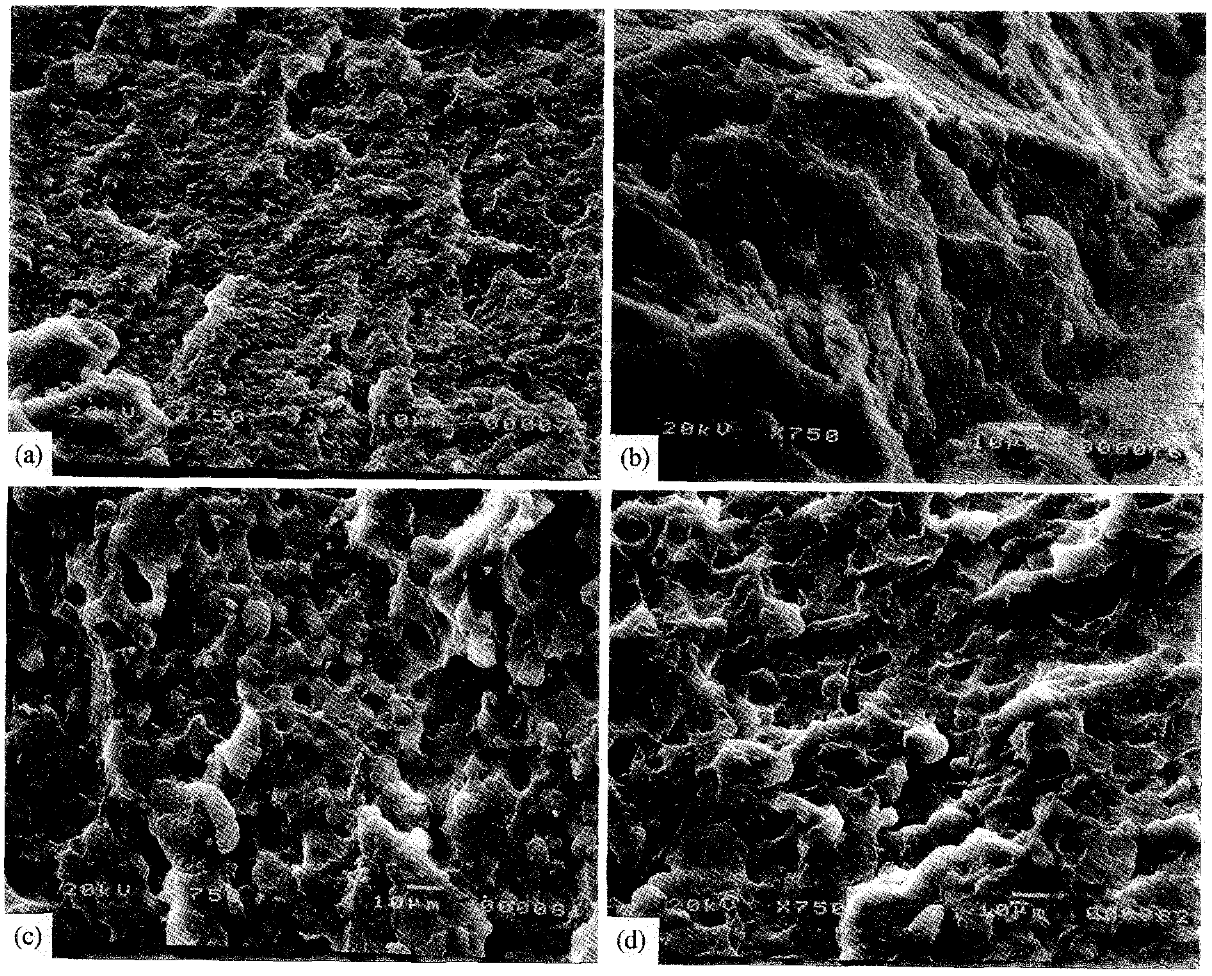

Figure 12 SEM micrographs of cryofractured ternary blends with indicated compatibilizers: (a) E-GMA; (b) E-EA-GMA; (c) SEBS-*g*-MA; (d) E-MeA-*g*-MA

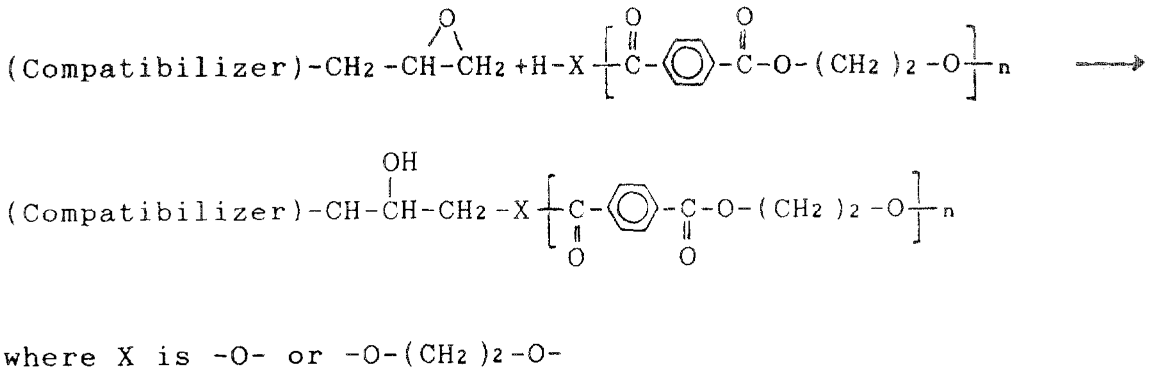

Scheme 1

into account various physical (rheology), physicochemical (interfacial tension) and chemical reactivity parameters. Not all of this information is available, however on the basis of the available data the following picture evolves. During REX, the compatibilizer with a polyolefinic chain is expected to mix with HDPE to give a nearly homogeneous blend, while the active groups (GMA or MA) participate in grafting reactions with the PET matrix. Hert[22], in discussing the toughening mechanisms of poly(butylene terephthalate) (PBT) with E-EA-*g*-MA or E-EA-GMA, demonstrated the higher reactivity of the GMA functionality compared to MA. In the former case, GMA may react with both carboxyl and hydroxyl terminal groups of the polyester (*Scheme 1*). On the other hand, MA may only react with the hydroxyl moieties and partly so because of the reversibility of the esterification reaction at the high mixing temperatures. Evidence for this was also the unchanging melt viscosity of PBT/E-EA-*g*-MA compared to pure PBT[22]. Although we do not have rheological data to support such a view, by analogy PET should behave in a similar way. Moreover, it was

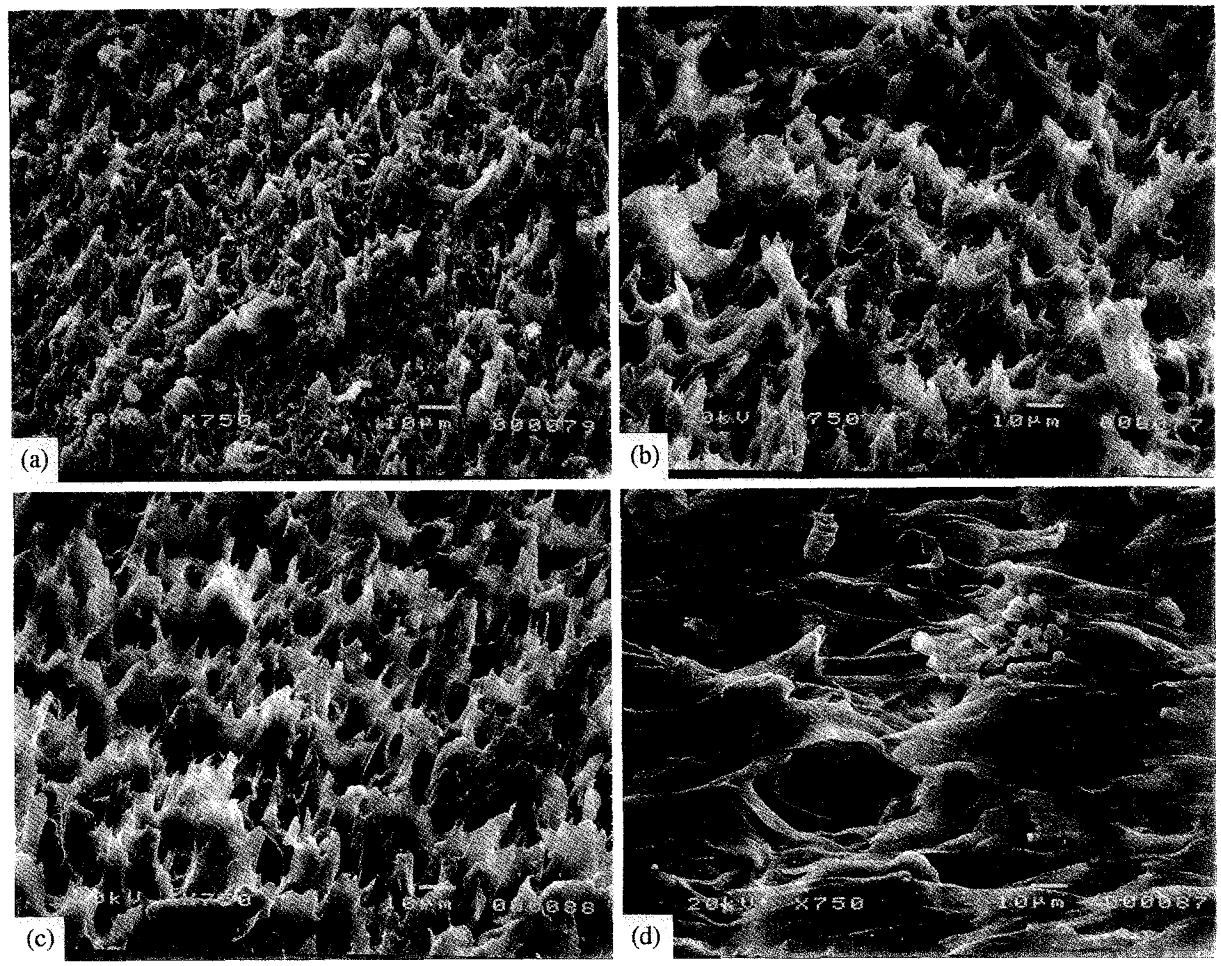

Figure 13 SEM micrographs of etched ternary blends with indicated compatibilizers: (a) E-GMA; (b) E-EA-GMA; (c) SEBS-*g*-MA; (d) E-MeA-*g*-MA

reported[23] that during compounding, the torque/throughput ratio was different for the four ternaries, decreasing along the ternary blend series E-GMA>E-EA-GMA>SEBS-*g*-MA>E-MeA-*g*-MA. A high value of this ratio signifies high melt viscosity. This could support the view that grafting efficiency decreases along the same sequence. If this is the case, then morphology evolution during REX would be different for the above ternaries. Thus in the case of GMA-containing compatibilizers, the dispersed HDPE+compatibilizer phase is more efficiently stabilized due to its higher reactivity (as explained above), and more uniform sub-micrometre sized domains are obtained. In the case of MA-containing compatibilizers, grafting reactions do not proceed to completion. Thus when the molten blend is not subjected to shearing, a fraction of the dispersed phase coalesces back into domains of larger average dimensions. As a result of this sequence of events, a morphology differentiation is obtained, the degree of dispersion becoming coarser along the ternary blend series E-GMA, E-EA-GMA, SEBS-*g*-MA, E-MeA-*g*-MA. This was indeed observed by optical microscopy and SEM. The SEBS-*g*-MA seems to be an exception, but it should be recalled that SEBS itself had an emulsifying capability for PET/HDPE blends[12].

Given the different blend morphologies, one can qualitatively explain the mechanical properties. Ultimate tensile properties, and especially energy to tensile failure E_b (see *Table 1*), depend on adhesion between the different phases in the compatibilized blend. The increased ability to disperse in GMA compatibilized ternaries leads to an increased interface across which grafting occurs, leading to improved tensile properties compared to blends obtained with MA compatibilizers. Again, SEBS-*g*-MA is an exception, which is tentatively attributed to its emulsification capability[24]. With regards to the impact strength variation (*Table 2*), the compatibilizers are grouped into two classes; E-GMA ternary blend >> the other three ternaries, which are equivalent in this respect. Also, the coarse E-MeA-*g*-MA ternary blend morphology does not seem to reduce impact strength as in the case of tensile properties. The explanation should be sought in the different mechanism of impact fracture. For PET this takes place by shear yielding and to a smaller extent by crazing. For such systems, Wu[25] has demonstrated that good adhesion between the dispersed phase and the matrix does not improve toughness. In a related study on PBT toughening, Hert[22] found a sub-micrometre narrow particle size distribution for the binary PBT/E-EA-GMA blend and a much higher impact strength value compared to a PBT/E-EA-*g*-MA binary, where size distribution was broad. In our case, the E-MeA-*g*-MA ternary blend has poor phase distribution; however, large particles, if cross-linked, may be effective in terminating crazing, thus contributing to the toughening mechanism[22]. Thus

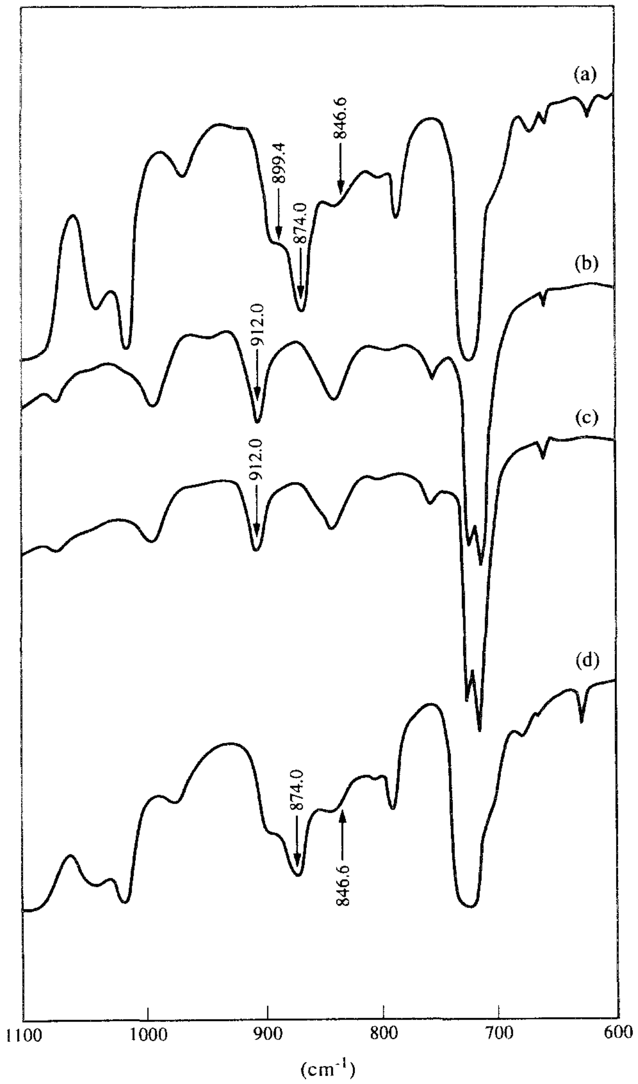

Figure 14 *FT*i.r. spectra of homopolymers and PET/E-GMA blends. (a) PET; (b) E-GMA; (c) E-GMA melt-treated at 280°C; (d) PET/E-GMA 70/30.

morphology differentiation is not so critical in this respect compared to tensile properties.

The main conclusions of this work are: (i) PET/HDPE (and possibly other POs as well) may be effectively compatibilized with REX using GMA and MA-containing compatibilizers; (ii) highest effectiveness is shown by the GMA compatibilizers, which is attributed to increased reactivity with the polyester terminal groups; (iii) morphology characterization and ultimate tensile properties are more discriminating in assessing compatibilizer efficiency compared to small deformation and impact properties.

ACKNOWLEDGEMENTS

This work was supported by a Brite Euram 0430-CT91 grant. The authors are indebted to the following individuals and companies: Dr A. Stassinopoulos and Dr E. Tsartolia, project coordinators from Argo S.A. (Greece); Cabot Plastics Ltd (UK) for material preparation and relevant information; research personnel from Fina Research S.A. and Spadel S.A. (Belgium) for useful discussions; Professor P. Koutsoukos for the use of the SEM facility.

REFERENCES

1 Howell, S. G. *J. Hazard. Mater.* 1992, **29**, 143
2 Boettcher, F.P. in 'Emerging Technologies in Plastics Recycling' (Eds G. D. Andrews and P. M. Subramanian), ACS Symposium Series No. 513, Washington, DC, 1992, Ch. 2
3 Bennett, R. A. in 'Emerging Technologies in Plastics Recycling' (Eds G. D. Andrews and P. M. Subramanian), ACS Symposium Series No. 513, Washington, DC, 1992, Ch. 3
4 Wilfong, D. L., Hiltner, A. and Baer, A. *J. Mater. Sci.* 1986, **21**, 2014
5 Wu, S. *Polym. Eng. Sci.* 1987, **27**, 335
6 Yokoyama, K., Fujita, Y., Higashida, N. and Inoue, T. *Makromol. Chem., Macromol. Symp.* 1994, **83**, 157
7 Subramanian, P. M. *Polym. Eng. Sci.* 1987, **27**, 1574
8 Subramanian, P. M. 'Compalloy' Conference Proceedings, SPE, New Orleans, 1990, p. 391
9 Akkapeddi, M. K. and Van Buskirk, B. Polymer Processing Society IX Annual Meeting, Manchester, 1993, p. 293
10 Kalfoglou, N. K. and Skafidas, D. S. *Eur. Polym. J.* 1994, **30**, 933
11 Kalfoglou, N. K., Skafidas, D. S. and Sotiropoulou, D. D. *Polymer* 1994, **35**, 3624
12 Traugott, T. D., Barlow, J. W. and Paul, D. R. *J. Appl. Polym. Sci.* 1983, **28**, 2947
13 Curry, J. and Kiani, A. 'SPE ANTEC 90', 1990, p. 1452
14 Wissler, G. E. 'SPE ANTEC 90', 1990 p. 1434
15 Carté, T. L. and Moet, A. *J. Appl. Polym. Sci.* 1993, **48**, 611
16 McCrum, N. G., Read, B. E. and Williams, G. 'Anelastic and Dielectric Effects in Polymeric Solids', Wiley, New York, 1967, p. 504
17 McCrum, N. G., Read, B. E. and Williams, G. 'Anelastic and Dielectric Effects in Polymeric Solids', Wiley, New York, 1967, p. 353
18 Utracki, L. A. 'Polymer Alloys and Blends', Hanser Publishers, Munich, 1989, Part 1
19 Paul, D. R. in 'Polymer Blends' (Eds D. R. Paul and S. Newman), Academic Press, New York, 1978, Vol. 2, Ch. 12
20 Akkapeddi, M. K. and Van Buskirk, B. *Polym. Mater. Sci. Eng.* 1992, **67**, 317
21 Xanthos, M. and Dagli, S. S. *Polym. Eng. Sci.* 1991, **31**, 929
22 Hert, M. *Angew. Makromol. Chem.* 1992, **196**, 89
23 Cabot Co Ltd, Plastics Division, UK
24 Chen, C. C. and White, J. L. *Polym. Eng. Sci.* 1993, **33**, 923
25 Wu, S. *Polymer* 1985, **26**, 1855